Journal of Thermal Analysis and Calorimetry, Vol. 91 (2008) 3, 723–731

NON-ISOTHERMAL CRYSTALLIZATION AND CRYSTALLINE STRUCTURE OF PP/POE BLENDS

J.-R. Ying[1,2], *S.-P. Liu*[1], *F. Guo*[1], *X.-P. Zhou*[1] *and X.-L. Xie* [1,3]*

[1]Hubei Key Laboratory of Materials Chemistry and Service Failure, Department of Chemistry and Chemical Engineering, Huazhong University of Science and Technology, Wuhan 430074, China
[2]Department of Chemical and Environment Engineering, Hubei University of Technology, Wuhan 430068, China
[3]State Key Laboratory of Plastic Forming Simulation and Die & Mould Technology, Wuhan 430074, China

Polypropylene (PP) /ethylene-octene copolymer (POE) blends with different content of POE were prepared by mixing chamber of a Haake torque rheometer. The crystallization behaviors and crystal structure of PP/POE blends were systematically investigated by differential scanning calorimetry (DSC), wide angle X-ray diffraction (WAXD) and polarized optical microscopy (POM). The results showed that PP spherulites became defective and the crystallization behavior was influenced intensely with the introduction of POE. At the low content of POE, the addition of POE decreases the apparent incubation period (Δt_i) and the apparent total crystallization period (Δt_c) of PP in blends due to the heterogeneous nucleation of POE, and small amount of β-form PP crystals form because of the existence of POE. However, at high content of POE, the addition of POE decreases the mobility of PP segments due to their strong intermolecular interaction and chain entanglements, resulting in retarding the crystallization of PP, decreasing in the amount of β-form PP crystals, and increasing in Δt_i and Δt_c of PP in blends.

Keywords: *crystal structure, non-isothermal crystallization, PP/POE blends*

Introduction

Isotactic polypropylene (PP) is a versatile commercial thermoplastic material with a wide range of domestic, automotive, construction and industrial applications [1]. However, PP is notch sensitive and poor impact resistance under severe conditions, such as at low temperatures and high impact rates, which has limited its applications in engineering fields. One of the efficient modifications is the incorporation of elastomers as toughening modifiers in PP matrix. The PP blends toughened by polyisobutene, polybutene-1, butadiene-styrene rubber (SBR), ethylene-vinyl acetate copolymer (EVA), ethylene-propylene rubber (EPR), ethylene-propylene-diene rubber (EPDM), styrene-ethylene-butadiene-styrene triblock copolymer (SEBS), polybutadiene and natural rubber were investigated [2–8]. Recently, ethylene/α-olefin copolymers, especially linear low density polyethylene (LLDPE) and ethylene-octene copolymers (POEs), have been produced by metallocene technology, and have attracted considerable attention due to the narrow molecular mass distribution, the high degree of comonomer, and their pellet form, which allows for faster mixing, broader handling and blending options [9–11]. Müller's [11] and Carriere's [12] groups investigated the effects of short-chain branching and comonomer type on the interfacial tension, nucleation and crystallization of blends of poly(propylene) and ethylene/α-olefin copolymers, respectively. Silva *et al*. [9, 10, 13] and McNally's group [14] studied the rheological, mechanical, thermal and morphological properties of PP/POE blends. Yang *et al*. [15] studied the brittle–ductile transition (BDT) behaviors of PP/POE blends in both impact and high speed tensile tests, and found that the notch sensitivity of the blends is essentially their tensile speed sensitivity. Zhang *et al*. [16] studied the effect of the nucleating agent (1,3,2,4-di(*p*-methyl-benzylidene) sorbitol (DM) on properties of POE toughened PP. They found that the addition of DM increases simultaneously the toughness and stiffness of the modified PP/POE blends at the same content of POE due to the low level of PP spherulites. Xu *et al*. [17] investigated the dispersion behavior of PP/POE blends by small-angle laser light scattering. Varga *et al*. [18–20] characterized the nucleating efficiency and selectivity of different β-nucleating agents of PP by DSC and temperature-modulated DSC, and investigated the influence of the blended polymer such as poly(vinylidene-fluoride) (PVDF), high density polyethylene (HDPE), random propylene copolymer (rPP), syndiotactic polypropylene (sPP) and polyamide 6 (PA6) on the formation of β-form crystals in PP. To our knowledge, no information about the crystallization and crystalline structure of PP/POE blends is valuable.

The mechanical properties of polymeric materials are controlled by microstructure, whilst their

* Author for correspondence: xlxie@mail.hust.edu.cn

1388–6150/$20.00
© 2008 Akadémiai Kiadó, Budapest
Akadémiai Kiadó, Budapest, Hungary
Springer, Dordrecht, The Netherlands

microstructure is remarkably influenced by the rheological parameters, melting and crystallization behaviors, and processing conditions. In the present, the non-isothermal crystallization behaviors and crystal structure of PP/POE blends were systematically studied.

Experimental

Materials and sample preparation

Isotactic PP (T36f) with a melt flow rate of 6.3 g/10 min (2.16 kg, 230°C) was supplied by Wuhan Petrochemical Co. Ltd., China. The POE (EG8150) was obtained from Du Pont Dow Elastomers Co. Ltd., USA, its melt flow rate is 0.9g/10 min (2.16 kg, 230°C). The POE mass fraction in PP/POE blends was 5, 10, 25, 30, 50 and 75%, and the resultant blends were designated as PP5, PP10, PP25, PP30, PP50 and PP75, respectively. In the preparation of the blends, PP and POE were melt-compounded using the mixing chamber (Rheomix 600) attachment connected to a Haake Torque Rheometer (Rheocord 90, Germany) operated at 210°C and 60 rpm for 6 min. The blends produced were then compression molded into plates under a pressure of 10 MPa at 190°C.

Methods

Differential scanning calorimetry (DSC)

DSC measurements were conducted in a Perkin-Elmer DSC-7 instrument at a heating rate of 10°C min^{-1} under dry nitrogen atmosphere. Prior to the DSC recording, all samples were heated to 190°C and then kept at this temperature for 5 min to eliminate the influence of their previous thermal histories. They were finally quenched to an ambient temperature. For nonisothermal crystallization measurement, the samples were heated to and kept at 190°C for 5 min [21], and then cooled to 25°C under different cooling rates of 5, 10, 20 and 30°C min^{-1}.

Wide-angle X-ray diffraction (WAXD)

A Philips X'Pert Pro X-ray Diffractometer with CuK_α radiation (λ=1.5406 Å) at a generator voltage of 40 kV and a current of 40 mA was used. The samples were cut from the above compression molded plates. All experiments were carried out in the 2θ range of 5–45° at ambient temperature with a scanning speed of 5° min^{-1} and step size of 0.02°.

Dynamic mechanical analysis (DMA)

DMA measurement was performed at a constant frequency 1 Hz and a heating rate of 3°C min^{-1} with a dynamic mechanical thermoanalyzer (Q800, TA instrument). The specimens with 35 mm length, 10 mm width and about 4 mm thickness were tested with dual cantilever clamp at temperature between –100 and 80°C.

Polarized optical microscopy (POM)

POM observation was performed by an Olympus BX 51 microscope equipped with a crossed polarizer and a hot stage. In order to observe the crystal morphology, the specimen was firstly melted at 200°C and kept at this temperature for 3 min, then quenched to the crystallization temperature (T_c=140°C) and maintained at T_c for the time necessary for isothermal crystallization.

Results and discussion

Melting behavior of PP/POE blends

Figure 1 shows heating DSC curves of PP and PP/POE blends at 5°C min^{-1}. The melting temperature (T_m, which is usually the end temperature of heating), the peak melting temperature (T_{mp}) and the onset of melting temperature ($T_{m,onset}$) are tabulated in Table 1. It can be seen that T_m, T_{mp} and $T_{m,onset}$ of PP in PP/POE blends all shift towards lower temperature with addition of POE. The depressions in melting temperature of PP phase in the blends indicate that there might be a strong intermolecular interaction between PP and POE according to Nishi–Wang theory [1, 22, 23].

Figure 2 shows the loss factor (*tan*δ) *vs*. temperature for PP, POE and PP/POE blends. It can be seen that neat PP and POE show one glass transition peak at 19.2 and –27.7°C, respectively. However the PP/POE blends exhibit two glass transition peaks. For

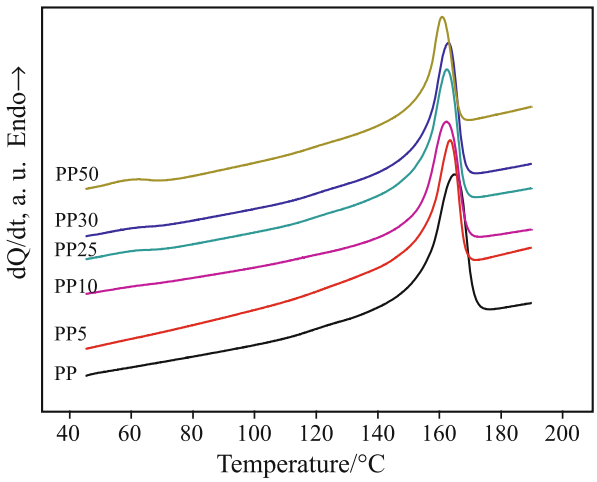

Fig. 1 Melting curves of PP and PP/POE blends at 5°C min^{-1}

Table 1 Melting temperature of PP phase in PP/POE blends measured at 20°C min^{-1}

	PP	PP5	PP10	PP25	PP30	PP50
T_{mp}/°C	165.0	163.4	162.2	162.5	162.9	160.9
T_m/°C	176.3	173.8	173.6	171.6	172.7	169.8
$T_{m,onset}$/°C	154.8	154.4	153.2	153.3	153.0	152.7

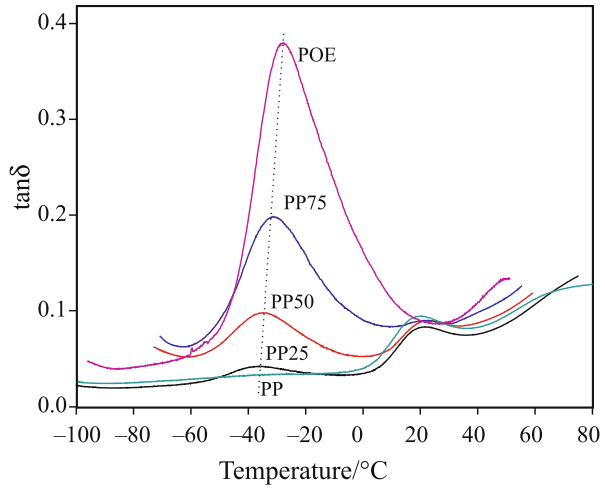

Fig. 2 Variation of loss factor with temperature for PP , POE and PP/POE blends

example, T_{g1} and T_{g2} of PP/POE 25/75 blend are located at about 22.2 and –31.3°C, respectively. This means that the blends are heterogeneous, i.e., PP and POE phases. Interestingly, with increasing POE content in blends, the glass transition peak of POE phase tends to shift towards high temperature and that of PP phase in blends tends to shift towards low temperature. These results all indicate that there are some interactions between PP and POE, and two polymers are partial compatible, which is consistent with the rheological results reported by McNally *et al*. [14].

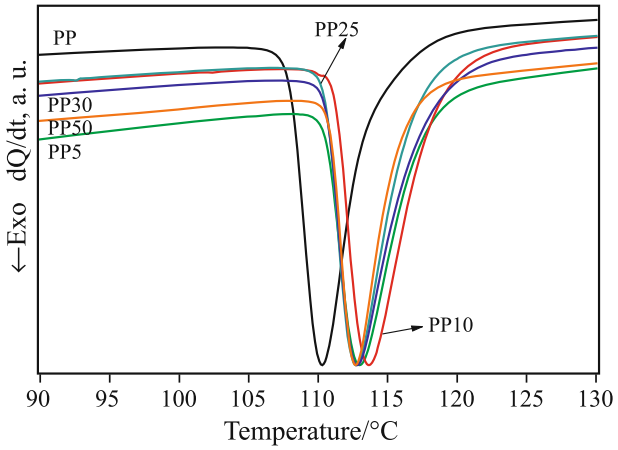

Fig. 3 Calorimetric crystallization curves of PP and PP/POE blends at 5°C min^{-1}

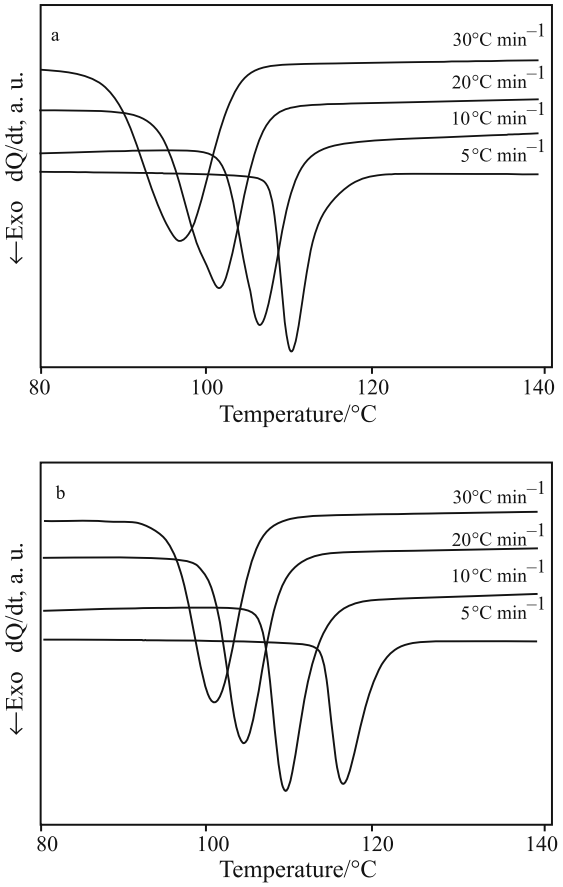

Fig. 4 Non-isothermal melt-crystallization exotherms of a – PP and b – PP5 at different cooling rate, ranging from 5 to 30°C min^{-1}

Non-isothermal crystallization behaviors of PP/POE blends

Figure 3 shows non-isothermal crystallization behaviors of PP and PP/POE blends at 5°C min^{-1}. It can be found that the crystallization peak and onset temperature of crystallization shift towards higher temperature, and the areas of exothermic curve decrease with increasing POE contents in the blends. It indicates that the crystallization of PP in blends is influenced by POE. Additionally, Fig. 4 is non-isothermal crystallization exotherms of PP and PP5 at different cooling rate ranging from 5 to 30°C min^{-1}. Other blends also exhibit the similar behaviors as PP5. Apparently, a single crystallization exotherm peak is observed at each cooling rate, and the exothermic peak trace

Table 2 Δt_i and T_{onset} of non-isothermal crystallization for PP and PP/POE blends

φ/°C min^{-1}	PP		PP5		PP10		PP25		PP30		PP50	
	T_{onset}/ °C	Δt_i/ min	T_{onset}/ °C	Δt_i/ min	T_{onset}/ °C	Δt_i/ min	T_{onset}/ °C	Δt_i/ min	T_{onset}/ °C	Δt_i/ min	T_{onset}/ °C	Δt_i/ min
5	123.9	13.2	126.0	12.8	127.5	12.5	126.1	12.8	127.0	12.6	124.2	13.2
10	122.6	6.8	123.8	6.6	124.7	6.5	125.0	6.5	122.5	6.8	120.5	7.0
20	116.4	3.7	117.2	3.6	122.0	3.4	120.0	3.5	118.0	3.6	114.0	3.8
30	113.0	2.6	115.3	2.5	119.0	2.4	117.0	2.4	116.0	2.5	113.0	2.6

becomes wider and shifts towards lower temperature with increasing cooling rate. This is because the crystallization is a slack process, in which polymer chains and segments rearrange and enter into crystal lattice, there exists a 'lag period' between crystallization process and temperature dropping (viz. non-isothermal crystallization is slower than temperature dropping), and the 'lag period' increases with increasing cooling rate. On the other hand, the movement ability of polymer chains and segments at lower temperature becomes weak, leading to the wider crystallization peaks.

Generally, the degree of supercooling ΔT is used to characterize the crystallization behavior of polymer melts [23–25], which is the difference between the equilibrium melting temperature T_m^0 and onset of the crystallization temperature T_{onset}. A decrease in ΔT indicates the decreasing in crystallization induce time of the crystallizing polymer. But ΔT can not accurately characterize the tendency of the total crystallization rate, and T_m^0 of polymer or blends can not be obtained easily. Thereby, Supaphol *et al*. [24, 25] proposed the apparent incubation period Δt_i and the apparent total crystallization period Δt_c to characterize quantitatively the induce time and the total crystallization rate, respectively.

Assuming the testing sample experiences the same thermal history, the arbitrary crystallization temperature T for non-isothermal crystallization can be converted to crystallization time t as following:

$$t = \left| T_{onset} - T/\varphi \right| \quad (1)$$

where φ is the specific cooling rate. According to Eq. (1), the apparent incubation period Δt_i can be defined as a time period during which the blend is still in its molten state, formulated as follows Eq. (2) [25]:

$$\Delta t_i = \left| T_f - T_{onset} \right| / \varphi \quad (2)$$

where T_f is the fusion temperature where the sample keeps molten state (in this experiment, T_f=190°C). The Δt_i values were calculated and are summarized in Table 2. For PP and PP/POE blends, it can be seen that Δt_i values monotonically decrease with increasing cooling rate. Figure 5 shows the relationship between the apparent incubation period Δt_i and POE content at various cooling rate. Apparently, the induce time at each cooling rate decreases with increasing the content of POE at low POE contents, but it increases with increasing the content of POE at high POE contents. It indicates that POE acts as a heterogeneous nucleating agent in PP/POE blends, resulting in accelerating the nucleation of PP during crystallization. However, the excessive POE retards the diffusion and packing of PP chains into crystal lattices, leading to increasing in induce time. In other word, there is a competition between nucleating and retarding crystallization of PP in PP/POE blends.

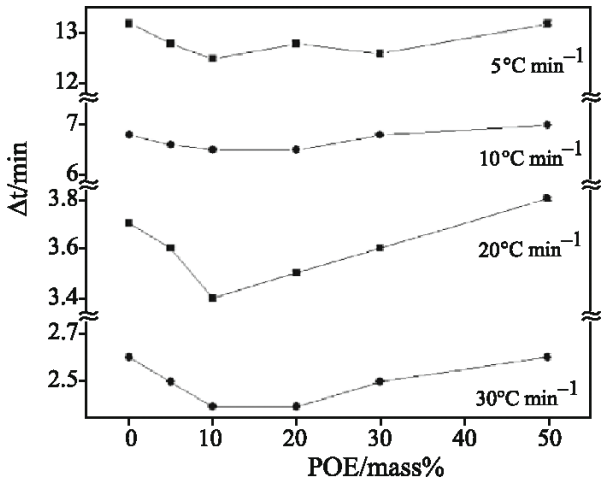

Fig. 5 Relationship between apparent incubation period Δt_i and POE content at different cooling rate

Based on the non-isothermal crystallization experiments, the enthalpy of crystallization as a function of temperature, dH_c/dT is obtained at different cooling rate. Thereby, the relative crystallinity as a function of temperature, θ(T), can be defined as follows equation [24, 25]:

$$\theta(T) = \frac{\int_{T_{onset}}^{T} (dH_c/dT)dT}{\Delta H_c} \in [0.1] \quad (3)$$

where T_{onset} and T denote the onset and arbitrary crystallization temperature during the crystallization process, respectively. ΔH_c is the total enthalpy of crystallization for an applied cooling rate. The relationship between relative crystallinity θ(T) and temperature T can be converted into the relative

crystallinity θ(t) as a function of time (Fig. 6). Apparently, the higher the cooling rate is, the less the time need for the crystallization process. Thereby, we can get $T_{0.01}$, $T_{0.1}$, $T_{0.25}$, $T_{0.5}$, $T_{0.75}$, $T_{0.9}$, $T_{0.99}$ and T_p, which represent the temperatures at 1, 10, 25, 50, 75, 90, 99% relative crystallinity, and the peak temperature at the maximum crystallization rate respectively. Some of those values for PP and blends are listed in Table 3. Similarly, the crystallization times, $t_{0.01}$, $t_{0.1}$, $t_{0.25}$, $t_{0.5}$, $t_{0.75}$, $t_{0.9}$ and $t_{0.99}$ at above relative crystallinity (t_θ) of PP and PP/POE blends at different cooling rate were calculated and are summarized in Table 4. It can be seen that t_θ values decrease with increasing cooling rate. Interestingly, for example, the logt_θ–logφ plots for PP5 (Fig. 7)

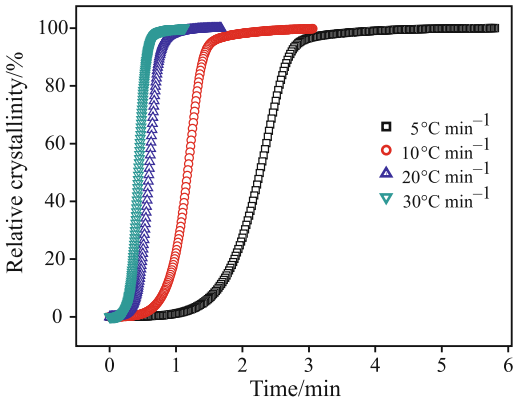

Fig. 6 Relative crystallinity as a function of time of PP5 observed at different cooling rate

Table 3 Temperature at different relative crystallinity for PP and blends

φ/°C min^{-1}	PP			PP5			PP10		
	T_p/°C	$T_{0.01}$/°C	$T_{0.99}$/°C	T_p/°C	$T_{0.01}$/°C	$T_{0.99}$/°C	T_p/°C	$T_{0.01}$/°C	$T_{0.99}$/°C
5	110.3	118.8	101.4	113.0	120.1	105.3	113.7	117.8	105.2
10	106.5	110.1	90.8	109.4	113.1	94.5	109.4	117.5	103.4
20	101.6	108.4	88.2	104.6	110.1	92.7	104.5	111.6	89.4
30	96.8	101.3	78 2	100.7	104.4	86.7	101.9	109.6	91.8
		PP25			PP30			PP50	
5	112.7	120.3	103.2	112.8	121.6	105.3	112.7	117.5	101.7
10	109.6	118.1	101.6	109.0	16.1	99.0	109.6	115.4	100.7
20	104.5	111.1	94.7	104.0	110.4	93.8	104.5	109.9	93.9
30	100.3	108.3	89.1	101.3	108.4	89.5	100.5	106.4	86.6

Table 4 Total crystallization period and crystallization time at different relative crystallinity

	φ/°C min^{-1}	Δt_c/min	$t_{0.01}$/min	$t_{0.1}$/min	$t_{0.25}$/min	$t_{0.5}$/min	$t_{0.75}$/min	$t_{0.9}$/min	$t_{0.99}$/min
PP	5	3.49	1.09	1.94	1.39	2.69	2.93	3.11	4.58
	10	1.93	0.66	1.15	1.33	1.49	1.66	1.81	2.59
	20	1.01	0.32	0.50	0.60	0.70	0.82	0.94	1.33
	30	0.77	0.26	0.39	0.46	0.55	0.64	0.74	1.03
PP5	5	2.97	0.97	1.64	1.97	2.26	2.51	2.70	3.94
	10	1.86	0.48	0.85	1.02	1.18	1.30	1.42	2.34
	20	0.87	0.24	0.43	0.51	0.59	0.67	0.75	1.11
	30	0.59	0.19	0.32	0.38	0.44	0.50	0.57	0.78
PP10	5	3.28	0.95	1.71	2.07	2.41	2.67	2.87	4.23
	10	1.40	0.42	0.82	1.02	1.18	1.30	1.40	1.82
	20	1.11	0.29	0.48	0.56	0.64	0.73	0.82	1.40
	30	0.59	0.20	0.34	0.40	0.46	0.52	0.58	0.79
PP25	5	3.42	0.95	1.69	2.03	2.34	2.56	2.75	4.37
	10	1.65	0.46	0.85	1.06	1.24	1.37	1.47	2.11
	20	0.82	0.25	0.43	0.50	0.58	0.65	0.72	1.07
	30	0.64	0.22	0.36	0.43	0.49	0.56	0.64	0.86
PP30	5	3.26	1.01	1.83	2.24	2.58	2.84	3.03	4.27
	10	1.71	0.49	0.87	1.03	1.17	1.29	1.41	2.20
	20	0.83	0.25	0.42	0.49	0.57	0.65	0.74	1.08
	30	0.63	0.22	0.35	0.40	0.46	0.52	0.59	0.85
PP50	5	3.16	0.71	1.25	1.51	1.74	1.92	2.09	3.87
	10	1.47	0.41	0.70	0.83	0.95	1.05	1.14	1.88
	20	0.80	0.19	0.32	0.38	0.45	0.52	0.61	0.99
	30	0.66	0.19	0.30	0.35	0.40	0.47	0.56	0.85

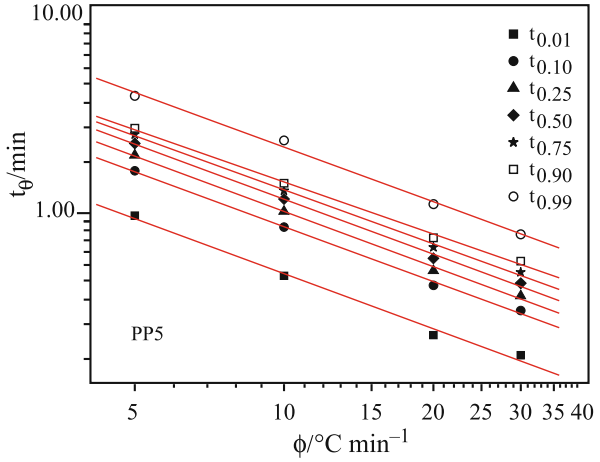

Fig. 7 Relationship between crystallization time and cooling rate for PP5

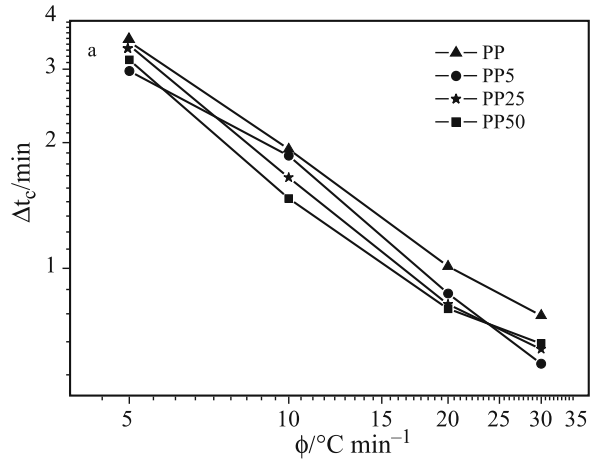

Fig. 8 Relationship between total crystallization period and POE content at different cooling rate

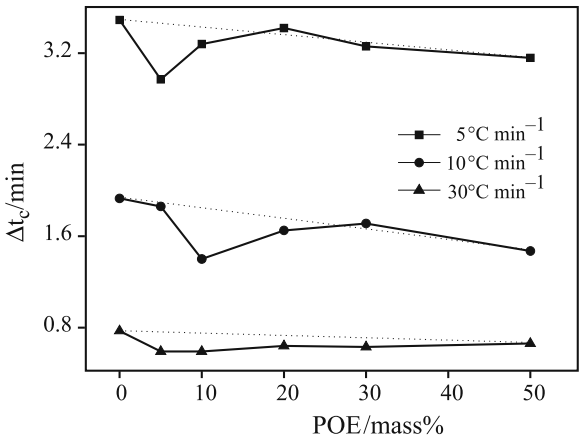

Fig. 9 Relationship between Δt_c and POE content at different cooling rate

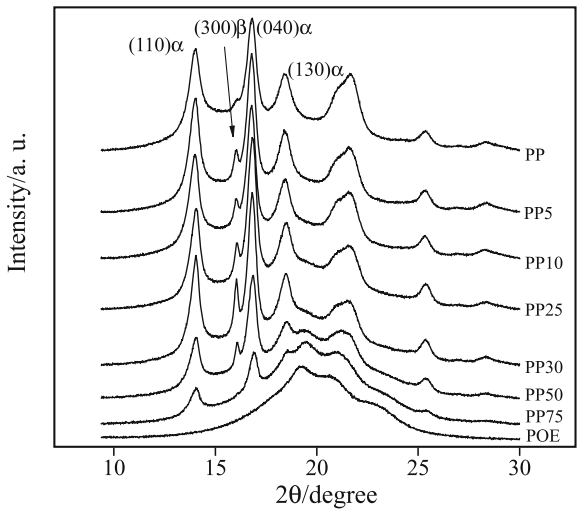

Fig. 10 WXRD curves of PP, POE and PP/POE blends

show excellent linearity, and their slopes at different relative crystallinity are almost equal.

Furthermore, in order to accurately measure the onset and the ending temperatures of the crystallization [25], $T_{0.01}$ and $T_{0.99}$ values are used to characterize the apparent onset and ending temperatures of the non-isothermal crystallization, approximatively. The apparent total crystallization period, Δt_c, can be calculated as follows:

$$\Delta t_c = t_{0.99} - t_{0.01} = (T_{0.01} - T_{0.99})/\varphi \qquad (4)$$

Figure 8 shows $\lg\Delta t_c$–$\lg\varphi$ plots of PP and PP/POE blends at different cooing rate. Apparently, their Δt_c values decreased with increasing the cooling rate, which implies that increasing cooling rate speed up the non-isothermal crystallization. Additionally, Fig. 9 shows the relationship between apparent total crystallization period (Δt_c) and POE content at different cooling rate. It can be seen that the addition of POE at the low content in PP/POE blends accelerates the crystallization of PP. However, at the high content of POE, the addition of POE retards the crystallization of PP in the blends, and increases the apparent total crystallization period. This is because that POE and PP is partially compatible; the heterogeneous nucleation of POE at low content enhances the crystallization of PP in the blends. However, at high content of POE, POE decreases the mobility of PP segments due to their strong intermolecular interaction and chain entanglements, resulting in retarding the crystallization of PP in the blends. The results are in accordance with the effect of POE on the above apparent incubation period of PP in the blends.

Crystal structure of PP/POE blends

The WXRD patterns of PP, POE and their blends are given in Fig. 10. The PP/POE blend, such as PP5, shows strong diffraction peaks at 14.01, 16.03, 16.78 and 18.42°. The peaks at 14.01, 16.78 and 18.42° correspond to [110], [040] and [130] diffractions of α-form PP crystals with a monoclinic configuration [1],

respectively. The peak at 16.03° is the characteristic [300] diffraction of the β-form PP crystals with a hexagonal configuration. This indicates that α-form and β-form PP crystals coexist in the PP/POE blends. With the addition of POE, the peak area and intensity of β-form crystals increase obviously. In order to study the crystal structure of the blends, peak-fit analyzing software was used to obtain a series of crystal parameters, such as interplanar space (d), half-width (β), apparent crystal size (L_{hkl}) etc. The degree of crystallinity (X_{all}) is given by:

$$X_{all} = \left(1 - \frac{A_a}{A_c + A_a}\right) \cdot 100\% \quad (5)$$

where A_a and A_c are the areas of the amorphous and the total crystal peaks, respectively. The k value corresponding to the fraction of the β-form crystal in the total crystalline phase is calculated from X-ray diffractograms according to Turner-Jones formula [26, 27]:

$$k = H_\beta / (H_{\alpha 1} + H_{\alpha 2} + H_{\alpha 3} + H_\beta) \quad (6)$$

where $H_{\alpha 1}$, $H_{\alpha 2}$, $H_{\alpha 3}$ are the intensities of [110], [040], [130] diffractions of α-form crystal, respectively. H_β is the intensity of [300] diffraction of β-form crystal.

The interplanar spacing (d) and apparent crystal size (L_{hkl}) values for the different peaks can be calculated by Bragg's law and Scherrer's formula [28], respectively.

$$d = \frac{\lambda}{2\sin\theta} \quad (7)$$

$$L_{hkl} = \frac{k'\lambda}{\beta_0 \cos\theta} \quad (8)$$

$$\beta_0 = \sqrt{\beta^2 - b_0^2} \quad (9)$$

where β_0 is the half-width of the reflection corrected for the instrumental broadening according to Eq. (8), β is the half-width of various diffraction peaks, b_0 is the instrumental broadening factor (0.15°), λ is the wavelength of radiation used, and k' is the instrument constant (0.9).

Table 5 summarizes the crystal structural parameters determined based on WAXD curves. The interplanar spacing d values for various peaks of PP in the blends show little change. The k value increases slightly with increasing the POE content, and yet the amount of β-form PP crystals in the blends tends to decrease at high content of POE. Similarly, $L_{(110)\alpha}$, $L_{(040)\alpha}$, $L_{(130)\alpha}$, $L_{(300)\beta}$ of α- and β-form crystals in PP/POE blends exhibit the same tendency as the formation of β-form PP crystals in the blends. These indicate that POE acts as a heterogeneous nucleating agent to α-form crystals, and induces a few the formation of β-form crystals. Generally, the β-form crystals may result from the fast cooling or from shearing during the compression molding [1]. Since PP and PP/POE blends are compression molded in the same process conditions, the inducing effect of

Table 5 WXRD data of PP and PP/POE blends

Sample	Diffractiom peak	2θ/°	d/Å	β_0/°	L_{hkl}/Å	k	X_{all}/%
PP	(110)α	14.01	6.32	0.55	141	0.156	68.4
	(300)β	16.06	5.51	0.29	245		
	(040)α	16.80	5.27	0.45	169		
	(130)α	18.42	4.81	0.74	106		
PP5	(110)α	14.01	6.32	0.52	149	0.162	52.1
	(300)β	16.03	5.52	0.19	330		
	(040)α	16.78	5.28	0.41	183		
	(130)α	18.42	4.81	0.57	137		
PP10	(110)α	13.99	6.33	0.51	152	0.164	48.4
	(300)β	16.03	5.52	0.22	296		
	(040)α	16.78	5.28	0.41	185		
	(130)α	18.42	4.81	0.55	142		
PP25	(110)α	14.04	6.30	0.48	158	0.167	45.4
	(300)β	16.06	5.51	0.22	305		
	(040)α	16.82	5.27	0.42	181		
	(130)α	18.49	4.79	0.54	144		
PP30	(110)α	14.04	6.30	0.47	163	0.195	44.4
	(300)β	16.03	5.52	0.16	361		
	(040)α	16.82	5.27	0.41	188		
	(130)α	18.47	4.80	0.54	143		
PP50	(110)α	14.04	6.30	0.55	140	0.188	28.6
	(300)β	16.08	5.51	0.16	371		
	(040)α	16.83	5.26	0.40	186		
	(130)α	18.52	4.77	0.46	165		

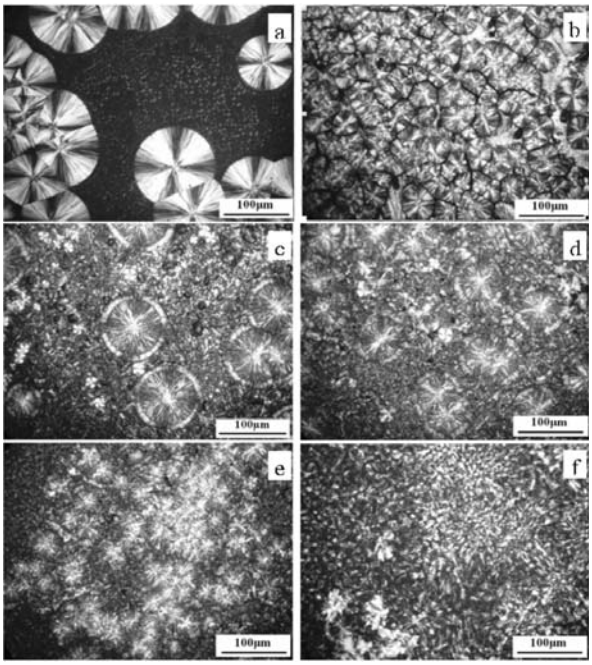

Fig. 11 POM micrographs of a – PP, b – PP5, c – PP10, d – PP25, e – PP30 and f – PP50

POE on the formation of β-form crystals in blends may be related to the changing in their rheological or crystallization behaviors due to the incorporation of POE. From Table 5, the amount of β-form crystals is small, so the melting peak of β-form crystals at approx. 155°C can not be found in Fig. 1. Additionally, the excessive POE retards the crystallization of PP in the blends and introduces the defects in crystals due to the formation of entanglements between POE and PP. The defect crystals can be found easily in the POM micrographs in Fig. 11c–f with 10–50 mass% POE contents. The decreasing in degree of crystallinity (X_{all}) for PP in the blends further confirms that effect of POE (Table 5).

POM micrographs of PP and PP/POE blends are shown in Fig. 11. The neat PP exhibits a common spherulitic structure with a diameter of 80 μm or more. With the addition of POE, the size of PP spherulites tends to decrease, and the β-form crystals are clearly seen in POM micrographs of PP/POE blends. It is worthy-mentioned that the quantities of PP spherulites in PP5 (with 5% POE content) are more than those in neat PP. This corroborates the fact that POE might play a heterogeneous nucleating role in PP/POE blends.

Conclusions

Based on the above results, we can conclude that with the introduction of POE, PP spherulites became defective and the crystallization behavior was influenced intensely. The apparent incubation period (Δt_i) and the apparent total crystallization period (Δt_c) can be used to characterize the crystallization behaviors of polymer blends. The results showed that at the low content of POE, the addition of POE decreases the Δt_i and Δt_c of PP in blends due to the heterogeneous nucleation of POE, and small amount of β-form PP crystals formed in blends because of the presence of POE. However, at high content of POE, the addition of POE decreases the mobility of PP segments due to their strong intermolecular interaction and chain entanglements, resulting in retarding the crystallization of PP and increasing in apparent incubation period and the apparent total crystallization period of PP in blends.

Acknowledgements

This work was supported by the National Natural Science Foundation of China (No. 20490220) and the Open Fund of State Key Laboratory of Plastic Forming Simulation and Die & Mould Technology of HUST (No. 05-10).

References

1 J. Varga, Polypropylene: Structure, Blends and Composites, J. Karger-Kocsis, (Ed.), Chapmann and Hall, London 1995 Vol. 1, pp. 56–115.
2 L. A. Utracki and M. M. Duomulin, Polypropylene: Structure, Blends and Composites, J. Karger-Kocsis, (Ed.), Chapmann and Hall: London 1995 Vol. 2, pp. 50–94.
3 A. K. Gupta, B. K. Ratnam and K. R. Srinivasan, J. Appl. Polym. Sci., 45 (1992) 1303.
4 R. Greco, G. Manearella, E. Martuscelli, G. Ragosta and J. H. Yin, Polymer, 28 (1987) 1929.
5 Y. Wang, Q. Zhang, B. Na, R. N. Du, Q. Fu and K. Z. Shen, Polymer, 44 (2003) 4261.
6 A. K. Gupta and S. N. Punwar, J. Appl. Polym. Sci., 31 (1986) 535.
7 L. K. Yoon, C. H. Choi and B. K. Kim, J. Appl. Polym. Sci., 56 (1995) 239.
8 W. Kaminsky, Macromol. Chem. Phys., 197 (1996) 3907.
9 A. L. N. D. Silva, M. C. G. Rocha, F. M. B. Coutinho and R. Bretas, J. Appl. Polym. Sci., 75 (2000) 692.
10 A. L. N. D. Silva, M. I. B. Tavares, D. P. Politano and F. M. B. Coutinho, J. Appl. Polym. Sci., 66 (1997) 2005.
11 A. C. Manaure and A. J. Müller, Macromol. Chem. Phys., 201 (2000) 958.
12 C. J. Carriere and H. C. Silvis, J. Appl. Polym. Sci., 66 (1997) 1175.
13 A. L. N. D. Silva, M. C. G. Rocha, F. M. B. Coutinho and R. E. S. Bretas, J. Appl. Polym. Sci., 79 (2001) 1634.
14 T. McNally, P. McShane, G.M. Nally, W. R. Murphy, M. Cook and A. Miller, Polymer, 43 (2002) 3785.
15 J. H. Yang, Y. Zhang and Y. X. Zhang, Polymer, 44 (2003) 5047.
16 X. F. Zhang, F. Xie, Z. L. Pen, Y. Zhang and Y. X. Zhang, Eur. Polym. J., 38 (2002) 1.
17 X. H. Xu, Y. B. Xu, X. Y. Yu, Y. J. Xu and J. Shen, J. Tianjin Univ., 39 (2006) 501.

18 A. Menyhárd, J. Varga and G. Molnár, J. Therm. Anal. Cal., 83 (2006) 625.
19 J. Varga and A. Menyhárd, J. Therm. Anal. Cal., 73 (2003) 735.
20 J. Varga and A. Menyhárd, Eur. Polym. J., 41 (2005) 669.
21 M. Avella, S. Cosco, M. L. Di Lorenzo, E. Di Pace and M. E. Errico, J. Therm. Anal. Cal., 80 (2005) 131.
22 O. Olabisi, L. M. Robeson and M. T. Shaw, Polymer-Polymer Miscibility, Academic Press, New York 1979.
23 X. L. Xie, K. Aloys, X. P. Zhou and F. D. Zeng, J. Therm. Anal. Cal., 74 (2003) 317.
24 P. Supaphol and J. Lin, Polymer, 42 (2001) 9617.
25 P. Supaphol, P. Thanomkiat and R. A. Phillips, Polym. Test., 23 (2004) 881.
26 A. Turner-Jones, J. M. Aizlewood and D. R. Beckett, Macromol. Chem., 75 (1964) 134.
27 J. Varga, J. Therm. Anal., 35 (1989) 1891.
28 L. E. Alexander, X-ray Diffraction Methods in Polymer Science; Wiley Interscience, New York 1969 P137.

Received: June 5, 2007
Accepted: October 3, 2007

DOI: 10.1007/s10973-007-8586-6